Journal Pre-proof

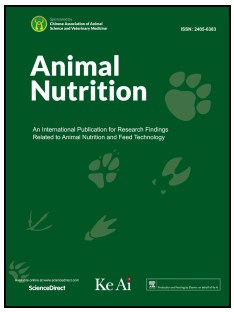

Inhibition of pyruvate dehydrogenase kinase improves carbohydrate utilization in Nile tilapia by regulating PDK2/4-PDHE1α axis and insulin sensitivity

Yuan Luo, Wenhao Zhou, Ruixin Li, Samwel M. Limbu, Fang Qiao, Liqiao Chen, Meiling Zhang, Zhen-Yu Du

PII: S2405-6545(22)00079-8

DOI: https://doi.org/10.1016/j.aninu.2022.06.011

Reference: ANINU 619

To appear in: *Animal Nutrition Journal*

Received Date: 7 December 2021

Revised Date: 5 May 2022

Accepted Date: 17 June 2022

Please cite this article as: Luo Y, Zhou W, Li R, Limbu SM, Qiao F, Chen L, Zhang M, Du Z-Y, Inhibition of pyruvate dehydrogenase kinase improves carbohydrate utilization in Nile tilapia by regulating PDK2/4-PDHE1α axis and insulin sensitivity, *Animal Nutrition Journal*, https://doi.org/10.1016/j.aninu.2022.06.011.

Author contributions

Zhenyu Du and **Yuan Luo** designed the experiments; **Yuan Luo** carried out the experimental work. **Yuan Luo** wrote the manuscript under the direction of **Zhenyu Du**. **Wenhao Zhou**, **Ruixin Li** and **Fang Qiao** assisted with the experimental work. **Samwel M Limbu**, **Liqiao Chen** and **Meiling Zhang** contributed to critical revision of the manuscript.

Inhibition of pyruvate dehydrogenase kinase improves carbohydrate utilization in Nile tilapia by regulating PDK2/4-PDHE1α axis and insulin sensitivity

Yuan Luo[a], Wenhao Zhou[a], Ruixin Li[a], Samwel M. Limbu[b,c], Fang Qiao[a], Liqiao Chen[a], Meiling Zhang[a], Zhen-Yu Du[a,d *]

[a] LANEH, School of Life Sciences, East China Normal University, Shanghai 200241, China

[b] University of Dar es Salaam, Department of Aquaculture Technology, Dar es Salaam 60091, Tanzania

[c] UDSM-ECNU Joint Research Center for Aquaculture and Fish Biology (JRCAFB), Dar es Salaam 60091, Tanzania

[d] ECNU-UDSM Joint Research Center for Aquaculture and Fish Biology (JRCAFB), Shanghai 200241, China

* Corresponding author.

E-mail address: zydu@bio.ecnu.edu.cn (Z. Du)

ABSTRACT

Pyruvate dehydrogenase kinases (PDKs)-pyruvate dehydrogenase E1α subunit (PDHE1α) axis plays an important role in regulating glucose metabolism in mammals. However, the regulatory function of PDKs-PDHE1α axis in the glucose metabolism of fish is not well known. This study determined whether PDKs inhibition could enhance PDHE1α activity, and improve glucose catabolism in fish. Nile tilapia fingerlings (1.90 ± 0.11 g) were randomly divided into 4 treatments in triplicate (30 fish each) and fed with control diet without dichloroacetate (DCA0) (38% protein, 7% lipid and 45% corn starch) and the control diet supplemented with DCA, which inhibits PDKs through binding the allosteric sites, at 3.75 (DCA3.75), 7.50 (DCA7.50) and 11.25 g/kg (DCA11.25), for 6 wk. The results showed that DCA3.75, DCA7.50 and DCA11.25 significantly increased weight gain, carcass ratio and protein efficiency ratio ($P < 0.05$) and reduced feed efficiency ($P < 0.05$) of Nile tilapia. To investigate the effects of DCA on growth performance of Nile tilapia, we selected the lowest doseDCA3.75 for subsequent analysis. Nile tilapia fed on DCA3.75 significantly reduced the mesenteric fat index, serum and liver triglyceride concentration and total lipid content in whole fish, and down-regulated the expressions of genes related to lipogenesis ($P < 0.05$) compared to the control. The DCA3.75 treatment significantly improved glucose oxidative catabolism and glycogen synthesis in the liver, but significantly reduced the conversion of glucose to lipid ($P < 0.05$). Furthermore, the DCA3.75 treatment significantly decreased the PDK2/4 gene and protein expressions ($P < 0.05$), accordingly stimulated PDHE1α

activity by decreasing the phosphorylated PDHE1α protein level. In addition, DCA3.75 treatment significantly increased the phosphorylated levels of key proteins involved in insulin signaling pathway and glycogen synthase kinase 3β ($P < 0.05$). Taken together, the present study demonstrates that PDK2/4 inhibition by using DCA promotes glucose utilization in Nile tilapia by activating PDHE1α, and improving insulin sensitivity. Our study helps to understand the regulatory mechanism of glucose metabolism for improving dietary carbohydrate utilization in farmed fish.

Keywords: Dichloroacetate; Glucose utilization; Insulin sensitivity; Nile tilapia; PDK2/4-PDHE1α axis

1. Introduction

Carbohydrates are abundant plant ingredients, and are generally considered as the most economical energy source in omnivorous and herbivorous fish nutrition, because of their relatively low cost and protein-sparing effect (Kamalam et al., 2017; Shrestha et al., 2011). Thus, increasing carbohydrate percentages in aquafeeds is one of the most economical nutritional strategies (Callet et al., 2020). Currently, high carbohydrate diets are widely used in aquaculture, especially in Nile tilapia (*Oreochromis niloticus*), gibel carp (*Carassius auratus* var. Gibelio), blunt snout bream (*Megalobrama amblycephala*) and grass carp (*Ctenopharyngodon idellus*) (Boonanuntanasarn et al., 2018a; Li et al., 2021; Limbu et al., 2020; Tan et al., 2009; Su et al., 2021; Shi et al., 2018). Fish species possess the key metabolic pathways and complete enzymatic systems for glucose catabolism (Kamalam et al., 2017). However, fish are poor users of dietary carbohydrates, and often display prolonged

hyperglycemia, excessive fat accumulation, growth retardation, reduced feed utilization, decreased antioxidant ability and immune functions after feeding them with high carbohydrate diets for a long period (Jin et al., 2014; Li et al., 2021; Xu et al., 2018). Although the precise reasons for poor utilization of carbohydrates by fish are not fully understood, it has been suggested that the low capacity of fish to use efficiently carbohydrate for energy is caused partly by the imbalance between the glucose breakdown (glycolysis and tricarboxylic acids [TCA] cycle) and synthesis (gluconeogenesis) (Hemer et al., 2002 ; Kamalam et al., 2017). Therefore, promoting complete glucose catabolism in fish, especially those fed on high carbohydrate diets, is an important research topic for fish nutritionists.

Activities for living animals depend on the availability of energy in the form of adenosine triphosphate (ATP), delivered from substrate fuels through the oxidative phosphorylation process (Stacpoole, 2017). Glucose is initially converted into pyruvate through several glycolytic intermediates in cytoplasm. On one hand, pyruvate is converted to acetyl-coenzyme A (acetyl-CoA) in mitochondria, which then enters the TCA cycle and oxidative phosphorylation to produce ATP, CO_2 and H_2O (Pithukpakorn, 2005). Moreover, pyruvate is also converted to other 3-carbon molecules for the synthesis of fatty acids and steroids (Wahren and Ekberg, 2007). Therefore, the final metabolic fate of pyruvate determines the efficient use of glucose directly as an energy supply substance by animals. The rate of glucose-derived pyruvate oxidation is dictated, in large part, by the multisubunit enzyme-pyruvate dehydrogenase (PDH) (Gudi et al., 1995; Takubo et al., 2013; Zhang et al., 2014),

which is the key enzyme system connecting glycolysis to the TCA cycle and the subsequent oxidative phosphorylation (Schafer et al., 2018; Wu et al., 2018a; Wu et al., 2000). PDH activity is regulated by reversible covalent modification via PDHE1α subunit (PDHE1α) phosphorylation, which is mediated by PDH kinases (PDKs) (Jeoung and Harris, 2008; Harris, 2002). Four PDK (PDK1-4) isoforms are expressed in a tissue-specific manner, with unique expression profiles in response to different physiological conditions (Wu et al., 2000). In mammals, PDK1 and PDK3 are mainly expressed in heart, kidney and testes. PDK2 and PDK4 are widely expressed in many tissues, including heart, brain, liver, islets, skeletal muscle and the adipose tissue (Klyuyeva et al., 2018; Wang et al., 2021). PDK1-4 are all serine-specific kinases, which can phosphorylate and inactivate PDHE1α, and among them PDK2 and PDK4 are the major PDKs, which are responsible for the regulation of PDHE1α activity in the liver (Harris et al., 2002; Jeoung and Harris, 2008). Similar to mammals, different PDK isoenzymes have been identified in common killifish (*Fundulus heteroclitus*) and zebrafish (*Danio rerio*) (Fukuda et al., 2020; Richards et al., 2008; Kuang et al., 2016). However, studies on the regulatory function of the PDKs-PDHE1α axis in glucose metabolism in Nile tilapia are currently lacking. PDKs-PDHE1α axis might be a potential regulatory target for improving the oxidative catabolism of glucose in fish.

Dichloroacetate (DCA) is a widely studied pyruvate mimetic, which inhibits PDKs through binding to the allosteric sites of PDK1, 2, 3 and 4 in mammals (Kato et al., 2007). By inhibiting the PDKs, the flux of pyruvate into the mitochondria is

increased, thus promoting glucose oxidation over glycolysis. Previous studies have indicated that DCA inhibited PDK4 expression, and activated PDHE1α expression by dephosphorylation at the serine 293 and 300 residues in mouse C2C12 cells (Thoudam et al., 2019) and H9C2 cardiac myocytes (Gopal et al., 2017). In normal and obese mice, DCA improved markedly glucose tolerance and insulin sensitivity, and enhanced total carbohydrate oxidation (Younghoon et al., 2016; Wu et al., 2018). In addition, DCA also increased glucose translocation and consumption in porcine intestinal epithelial (IPEC-J2) cells (An et al., 2018). In zebrafish, some studies showed that the DCA-mediated PDK2 inhibition reduced lactate production; DCA also inhibited PDK4, and induced a shift in energy supply from fatty acids to glucose in cardiomyocytes (Fukuda et al., 2020; Kuang et al., 2016). Therefore, we hypothesized that DCA may act as an effector to improve the glucose utilization in fish by regulating the PDKs-PDHE1α axis.

Nile tilapia is one of the most important economic omnivorous species in global aquaculture (FAO, 2020). Generally, diets containing 300-350 g/kg carbohydrate do not affect Nile tilapia growth performance (Boonanuntanasarn et al., 2018b; Wang et al., 2005). Our previous studies showed that diets containing 450 g/kg carbohydrate led to excessive fat accumulation and reduced growth performance in Nile tilapia (Li et al., 2020b; Liu et al., 2018; Luo et al., 2020; Xu et al., 2021; Limbu et al., 2020). Normally, the adverse effects of high carbohydrate diets on Nile tilapia are ascribed to the imbalance between glucose catabolism for energy provision and conversion to fats (Liu et al., 2018; Prisingkorn et al., 2017). In the present study, Nile tilapia were fed

with a control diet containing 450 g/kg corn starch (DCA0), and the control diet supplemented with different concentrations of DCA at 3.75 (DCA3.75), 7.50 (DCA7.50) and 11.25 g/kg (DCA11.25) levels for 6 wk. The aim was to evaluate the regulatory roles of the PDKs-PDHE1α axis on the glucose utilization efficiency and fat accumulation in fish. Our study demonstrates that PDK2/4 inhibition by using DCA promoted glucose utilization in Nile tilapia by activating PDHE1α and improving the insulin sensitivity. These results help to understand the regulatory mechanism of glucose metabolism for improving energy supply from dietary carbohydrates for farmed fish. This is also the first study elucidating the potential regulatory function of the PDKs-PDHE1α axis in improving the carbohydrate utilization in fish.

2. Materials and Methods

2.1. Ethical statement

All experiments were conducted strictly under the Guidance Suggestions for the Care and Use of Laboratory Animals formulated by the Ministry of Science and Technology of China. In the present study, all the animal experimental procedures were conducted in compliance with the Ethics of Animal Experiments of East China Normal University (approval number F20210101).

2.2. Experimental fish, diets and study design

Nile tilapia (all-male) fingerlings were purchased from Bairong Fish Breeding Farm in Guangzhou, China. Before the formal trial, the fish were acclimated in a recirculating aquaculture system for 2 wk. During the acclimation process, fish were

fed a purified diet containing 380 g/kg protein, 50 g/kg lipid and 300 g/kg corn starch. Four isonitrogenous and isolipidic purified experimental diets were formulated, including a control diet (DCA0, 450 g/kg corn starch), and the control diet supplemented with 3 doses of DCA at 3.75 (DCA3.75), 7.50 (DCA7.50) and 11.25 g/kg (DCA11.25). Protein was supplied by casein and gelatin. Dietary lipid was supplied by soybean oil. Corn starch was used to provide the required dietary carbohydrate level. In our previous studies, 450 g/kg corn starch was used to formulate the high carbohydrate diets for Nile tilapia (Luo et al., 2020; Limbu et al., 2020). The diets contained approximately 380 g/kg protein and 70 g/kg lipid, which met the nutritional requirements of Nile tilapia according to our previous studies (Li et al., 2021; Limbu et al., 2020; Luo et al., 2020). Feed formulation and proximate composition of the diets used in the present study are presented in Table 1. The ingredients were finely ground, mixed homogeneously, and pelletized by using a double helix plodder (F-26, SCUT industrial factory, Guangdong, China). The experimental diets were dried at 40 °C for 24 h, and stored at -20 °C until use. After the acclimation period, 360 Nile tilapia fingerlings with no exterior injuries and deformities (initial mean weight: 1.90 ± 0.11 g) were divided randomly into 12 tanks (each tank held 30 fish, in 3 replicates) in a recirculating aquaculture system. The size of each tank was 0.8 m × 0.6 m × 0.6 m (containing 250 L water), and the water flow rate was 200 L/h. The fish were hand-fed by using the four experimental diets twice a day (8:30 and 17:30 h) at a daily feeding rate of 4% body weight for 6 wk. The daily intake of DCA for fish was 0, 150, 300 and 450 mg/kg body weight, respectively. The

dietary DCA doses were determined based effective dosages already used in previous studies in rat and zebrafish (Wu et al., 2018; Hassoun et al., 2005). Body weight of all fish in each tank was bulk measured once every week by using an electronic weighing scale to adjust their daily feed rations. The remaining feeds after 1 h of feeding were siphoned, dried and weighed for the determination of feed intake. During the feeding trial period, the water temperature, pH, dissolved oxygen and ammonia nitrogen were 27.00 ± 2.00 °C, 7.80 ± 0.20, > 7.00 mg/L and < 0.05 mg/L, respectively.

2.3. Samples collection for analyses

At the end of the 6 wk feeding trial, all fish were fasted overnight and anaesthetized by using MS222 (20 mg/L). The survived fish in each tank were counted to determine their number and bulk weighed. Three fish per tank were sampled randomly and individually measured for their body weight and length. After weight and length measurements, blood was drawn from the caudal vein of the nine fish by using 2 mL syringes (Klmedical, China). Blood samples were immediately centrifuged at 1,000 × *g* for 10 min at 4 °C, the serum was placed into polypropylene tubes for biochemical analysis. The remaining fish after blood collection were dissected individually for collecting liver, muscle and mesenteric samples. The mesenteric fat and liver samples were weighed for organ indices analysis. The liver and muscle samples were instantly frozen in liquid nitrogen, and then stored at -80 °C for the analyses of glycogen and triglyceride (TG) contents and mRNA expression of genes. The fish head, fin and visceral were removed from all the 4 fish per tank (12 fish per treatment), and were weighed for the determination of carcass ratio. Another

196 6 fish from each treatment were randomly collected and stored at -20 °C for body
197 proximate composition analysis.

198 *2.4. Estimation of growth performance, survival rate, feed efficiency, and organ*
199 *indices*

200 The data obtained on weight, number of fish, length, amount of feed and organs
201 weight were used to compute growth performance, survival rate, feed efficiency, and
202 organ indices by using the following formulae:

203 Weight gain (WG, %) = 100 × [(final weight, g) – (initial weight, g)]/(initial
204 weight, g);

205 Survival rate (SR, %) = 100 × final fish number/initial fish number;

206 Feed conversion ratio (FCR) = (feed fed during the entire study, g)/ biomass
207 gained during the study, g;

208 Hepatosomatic index (HSI, %) = 100 × (liver weight, g)/(individual fish weight,
209 g);

210 Mesenteric fat index (%) = 100 × (mesenteric fat weight, g)/(individual fish
211 weight, g);

212 Feed intake (FI, %) = 100 × (dry feed consumed, g)/ {[(final weight, g) + (initial
213 weight, g)]/2}/d;

214 Protein efficiency ratio (PER) = (biomass gained during the study, g)/(total
215 protein intake, g DM);

216 Condition factor (CF, %) = 100 × (final weight, g)/(final body length, cm^3);

217 Carcass ratio (CR, %) = 100 × [(body weight, g) – (head weight, g) – (fin weight,

g) – (visceral weight, g)]/(body weight, g).

2.5. Biochemical parameters analyses

Specific commercial assay kits (Nanjing Jiancheng Bioengineering Institute, Nanjing, China) were used to measure the contents of TG (Kit F001-1) and glycogen (Kit A043-1) in the liver and muscle. Similarly, the concentrations of TG, glucose (Kit F006-1) and insulin (Kit H203-1) were analyzed in the serum by using specific commercial assay kits (Nanjing Jiancheng Bioengineering Institute, Nanjing, China). All measurement steps were performed according to the relevant kit protocols. Furthermore, the total lipid in the whole fish was extracted and determined by using the chloroform/methanol (2:1, vol:vol) method (Folch, 1957).

2.6. Total RNA extraction, cDNA synthesis and quantitative real-time PCR

Six fish were sampled for brain, heart, muscle, liver, kidney, spleen, gill, intestinal and adipose tissues collection for total RNA extraction using RNAiso Plus (Takara, Japan) according to the manufacturer's instructions. The quality and quantity of RNA were determined by agarose gel electrophoresis and Nanodrop 2000 spectrophotometer (Thermo Fisher Scientific, USA), respectively. The RNA was reverse transcribed to cDNA by using the PrimeScript Reagent kit (Takara, Japan). It was subsequently used to analyze the tissue expression specificity of PDK1/2/3/4 genes. Similarly, the liver and muscle tissues of 6 fish from each treatment were also collected for total RNA extraction, cDNA synthesis and quantitative real-time PCR (qRT-PCR). The elongation factor 1 alpha (*ef1α*) and *β-actin* were used as reference genes due to their stability for Nile tilapia (Limbu et al., 2018). The primers used in

the present study are showed in Table 2. The expression of genes was quantified by using qRT-PCR (Bio-rad, USA) with the SYBR qPCR reagent (Vazyme Biotech CO., Ltd. Nanjing, China). The qRT-PCR results were estimated by the $2^{-\Delta\Delta Ct}$ method (Livak and Schmittgen, 2001). In the present study, the qRT-PCR efficiency was between 95% and 105% for all analyses, and the correlation coefficient was over 0.96 for each gene. Each qRT-PCR run was performed in triplicate with negative control (no cDNA) also included.

2.7. Western blot analysis

The liver tissues from 9 fish from each treatment for western blot assays were prepared as reported by Luo et al. (2020). The liver protein concentrations were measured by using a bicinchoninic acid assay protein kit (Beyotime Biotechnology, China) to determine the loading volume. Express cast PAGE gel (New Cell & Molecular Biotech, China) was run using 50 μg of protein lysate per lane. The gels obtained were then transferred into nitrocellulose (NC) membranes for 90 min at 90 mV, and the NC membranes were blocked with 5% bovine serum albumin. The information on antibodies used for this study is provided in Table 3. The glyceraldehyde-3-phosphate dehydrogenase (Gapdh) was used as a reference protein. The detection and quantification were performed by using the Odyssey CLX Imager (LI-COR, Inc., USA).

2.8. Histological analysis

Small pieces (about 1 cm^3) of liver and muscle tissues were fixed in 4% paraformaldehyde (Servicebio Technology Co., Ltd. Wuhan, China) for 48 h at room

262 temperature. The fixed tissues were then embedded in paraffin wax, and were cut into
263 5 μm slices for periodic acid-Schiff (PAS) staining. The liver tissue was incubated by
264 using 30% sucrose at 4 °C for 72 h. The liver tissue was then embedded at optimum
265 cutting temperature compound (Sakura, Japan), and was immediately frozen at -80 °C
266 for oil red O (Sigma-Aldrich, USA) staining. The histological features were observed
267 and photographed by using a light microscope (Nikon Ds-Ri2, Japan).

268 *2.9. Glucose tolerance test (GTT)*

269 The glucose tolerance test (GTT) was performed as described in our previous
270 studies (Liu et al., 2018; Li et al., 2020a). After the feeding trial, 96 fish (24 fish per
271 treatment) were fasted for 12 h. The fish were then intraperitoneally (i.p.) injected
272 with 500 mg/kg of glucose. The fish from each treatment were then sampled at 0, 30,
273 60 and 180 min after the glucose injection (6 fish per time point) for tail vein blood
274 collection and the serum was immediately obtained as described in the previous
275 section. Glucose and insulin levels in serum samples were determined by using
276 specific kits as shown above.

277 *2.10 Metabolic tracking test of [1-^{14}C]-Glucose*

278 After the feeding experiment and overnight fasting, 6 fish from each treatment
279 were randomly collected and anesthetized with tricaine methane sulfonate (Western
280 Chemicals, Inc., Ferndale, USA) at 20 mg/L). The fish were i.p. injected with saline
281 containing [1-^{14}C]-glucose (500 mg/kg body weight and 0.1 M Bq per 50 g body
282 weight). The injected fish were moved immediately into a closed glass jar containing
283 the oxygen-saturated water, which was connected to another glass bottle containing

the 1 mol/L potassium hydroxide (KOH) solution. The details of the experimental process on metabolic tracking test of [1-^{14}C]-glucose were as previously described (Yoshida and Harper, 1960; Garin et al., 1987). Briefly, 1 mol/L KOH solution absorbs $^{14}CO_2$ released from the oxidation of the [1-^{14}C]-glucose. The $^{14}CO_2$ released was collected during the 90 min release period. The liver and muscle samples (0.5 g) were digested by using a digestion solvent (30% H_2O_2/$HClO_4$, 1:2, vol/vol) (1:5, w/vol) at 60 °C in a water bath for 6 h. The ^{14}C-protein (the 1 mmol/L NaCl-Tris-HCl/10% $HClO_4$ extraction method), ^{14}C-lipid (the chloroform-methanol extraction method, 2:1, vol/vol) and ^{14}C-glycogen (the 70% ethanol precipitation method) were extracted as described previously (Challiss et al., 1983; Chan and Krebs, 1985; Li et al., 2020a; Li et al., 2020b; Li et al., 2021). After the extraction, the ^{14}C-labeled macronutrients were dissolved into 0.5 mL of strong lysate (30% H_2O_2/$HClO_4$, 1:2, vol/vol). The radioactivity of 200 μL KOH solution and nutrient lysate were measured after mixing with 2 mL scintillation fluid (Ultima Gold XR, Packard, USA) by using the Tri-Carb 4910TR Liquid Scintillation Analyzer (PerkinElmer, USA).

2.11. Statistical analyses

All data were tested for normality by using the Kolmogorov-Smirnov test while homogeneity of variances was determined by using the Levene's test. The significant differences on final body weight (FBW), WG, SR, FCR, FI, PER, CF and CR among the DCA0, DCA3.75, DCA7.50 and DCA11.25 treatments were all tested by using one-way analysis of variance (ANOVA) followed by the Tukey's multiple comparison

test for specific differences. The significant differences of the remaining measured parameters between the DCA0 and DCA3.75 treatments were all evaluated by using the independent *t*-test. Results with $P < 0.05$ were considered statistically significant. All results are reported as means ± standard error of the mean (SEM) as indicated in figure legends. All statistical analyses were performed by using the GraphPad Prism 7.0 software (GraphPad Software Inc., La Jolla, CA, USA).

3. Results

3.1. The effects of DCA on growth performance and feed efficiency

After the 6 wk feeding trial, the Nile tilapia fed on the DCA3.75, DCA7.50 and DCA11.25 diets had significantly higher FBW, WG, PER and CR than those fed on the DCA0 diet ($P < 0.05$) (Fig. 1A, B, F, H). In addition, the Nile tilapia fed on the DCA3.75, DCA7.50 and DCA11.25 diets had significantly lower FCR than those fed on the DCA0 diet ($P < 0.05$) (Fig. 1D). However, feeding the Nile tilapia with all the experimental diets did not affect the SR, FI and CF ($P > 0.05$) (Fig. 1C, E, G). Therefore, we selected the DCA3.75 treatment, which contained the lowest dose of DCA for subsequent analysis.

3.2. The effects of DCA on lipid deposition

In the present study, we analyzed lipid deposition-related parameters. The results showed that, feeding the Nile tilapia with the DCA3.75 diet significantly reduced the mesenteric fat index, TG concentration in the serum, total lipid in the whole fish, lipid droplets amount in the liver, and TG level in the liver ($P < 0.05$) (Fig. 2B-F). However, feeding the Nile tilapia with the DCA0 and DCA3.75 diets did not affect the HSI ($P >$

0.05) (Fig. 2A). Interestingly, Nile tilapia fed on the DCA3.75 diet significantly reduced the expressions of genes related to lipid synthesis, such as sterol regulatory element binding transcription factor 1 (*srebp1*), fatty acid synthase (*fas*), diacylglycerol o-acyltransferase (*dgat*) and acetyl-coa carboxylase α (*accα*) ($P < 0.05$) (Fig. 2G). However, the DCA0 and DCA3.75 diets had no significant effect on the expressions of key genes involved in lipid catabolism in Nile tilapia, such as peroxisome proliferator activated receptor α (*pparα*), carnitine palmitoyl transferase 1b (*cpt1b*) and acetyl-coa carboxylase β (*accβ*) ($P > 0.05$) (Fig. 2G).

3.3. The effects of DCA on glucose metabolism

The Nile tilapia fed on the DCA3.75 diet had significantly lower glucose in the serum compared to those fed on the DCA0 diet ($P < 0.05$) (Fig. 3A). Feeding the fish with the DCA3.75 and DCA0 diets did not affect insulin concentration ($P > 0.05$) (Fig. 3B). The results for the GTT test showed that the DCA3.75-fed fish had a faster glucose clearance rate and a lower insulin concentration in the serum than those fed on the DCA0 diet ($P < 0.05$) (Fig. 3C, D). To gain insight into the role of DCA in the overall regulation of glucose metabolism in Nile tilapia, we tracked the use of [1-^{14}C]-glucose that had been i.p. injected (Fig. 3E). The results for the metabolic tracking test showed that the fish fed on the DCA3.75 diet had significantly higher $^{14}CO_2$ release (Fig. 3F) and ^{14}C-glycogen deposition (Fig. 3H) in the liver than those fed on the DCA0 diet ($P < 0.05$). However, the fish fed on the DCA3.75 diet had significantly lower ^{14}C-lipid content ($P < 0.05$) (Fig. 3G) in the liver than those fed on the DCA0 diet. The fish fed on the DCA3.75 diet had similar ^{14}C-protein deposition with those fed on the DCA0

diet (Fig. 3I). In the muscle, the deposition of ^{14}C-lipid (Fig. 3J), ^{14}C-glycogen (Fig. 3L) and ^{14}C-protein (Fig. 3K) were not significantly different between the fish fed on both diets ($P > 0.05$). The results for the PAS analysis showed that the fish fed on the DCA3.75 diet had higher glycogen content in the liver (Fig. 3M, N) accompanied with higher mRNA expression of glycogen synthase (*gs*) ($P < 0.05$) (Fig. 3O). However, glycogen content (Fig. 3P, Q) and mRNA expression of *gs* (Fig. 3R) in the muscle of Nile tilapia were not significantly different between the DCA3.75 and DCA0 treatments ($P > 0.05$).

3.4. The effects of DCA on the PDK2/4-PDHE1α axis and expression of genes related to glucose metabolism

The Nile tilapia fed on the DCA3.75 diet up-regulated the expressions of genes related to glucose transport (glucose transporter 2, *glut2*; glucose transporter 4, *glut4*) ($P < 0.05$) (Fig. 4A). Furthermore, the fish fed on the DCA3.75 diet up-regulated the expressions of glycolysis-related genes, including glucokinase (*gk*), phosphofructokinase (*pfk*) and pyruvate kinase (*pk*) (Fig. 4B), as well as citrate synthase (*cs*) (Fig. 4D) than those fed on the DCA0 diet ($P < 0.05$). However, the Nile tilapia fed on the DCA3.75 diet significantly down-regulated the mRNA expression of the gluconeogenesis related gene-phosphoenolpyruvate carboxykinase (*pepck*) than those fed on the DCA0 diet ($P < 0.05$) (Fig. 4C). The Nile tilapia fed on the DCA3.75 diet significantly increased the expressions of mitochondrial cytochrome c oxidase 1 (*mtco1*), succinate dehydrogenase complex subunit A (*sdha*) and NADH dehydrogenase [ubiquinone] 1a subcomplex subunit 9 (*nduta9*) ($P < 0.05$) (Fig. 4E).

We further analyzed the effects of DCA on the PDKs-PDHE1α axis, because it plays an important role in regulating the entry of glucose-derived pyruvate into the TCA cycle to generate acetyl-CoA. The results showed that the PDKs (*pdk1*, *pdk2*, *pdk3* and *pdk4)* were expressed widely in many organs, including brain, heart, muscle, liver, kidney, spleen, gill, intestine and the adipose tissue of Nile tilapia. In the liver, an important target organ of glucose metabolism, the mRNA and protein expressions of *pdk2* and *pdk4* gene were significantly higher than *pdk1* and *pdk3* ($P < 0.05$) (Fig. 4F, G). The Nile tilapia fed on the DCA3.75 diet had lower protein concentrations of Pdk2 and Pdk4 (Fig. 4H) with low mRNA expressions (Fig.4 J) in the liver compared to those fed on the DCA0 diet ($P < 0.05$). Likewise, the Nile tilapia fed on the DCA3.75 diet had lower protein concentration of p-Pdhe1α (Fig. 4H) than those fed on the DCA0 diet ($P < 0.05$). However, the total protein concentration of Pdhe1α and its mRNA expression were not significantly affected between the fish fed on the DCA3.75 and DCA0 diets in the liver ($P > 0.05$).

3.5. The effects of DCA on the insulin signaling and glycogen synthase kinase 3 beta (Gs3kβ) expression

The fish fed on the DCA3.75 diet significantly increased the phosphorylated protein levels of insulin receptor beta [Irβ (Tyr1345)], insulin receptor substrate 1 [Irs1 (Ser636/639)], phosphatidylinositol 3-kinase [Pi3k (Tyr458/198)] and serine/threonine kinase [Akt (Ser473)] compared with those fed on the DCA0 diet ($P < 0.05$) (Fig. 5A, B). However, the fish fed with the DCA3.75 diet did not significantly affect the total protein levels of Irβ, Irs1, Pi3k and Akt in the liver ($P >$

0.05). The fish fed on the DCA3.75 diet significantly increased the phosphorylated level of Gs3kβ at the site of ser9 ($P < 0.05$), but did not change its total protein content ($P > 0.05$) (Fig. 5C, D).

4. Discussion

4.1. Dietary DCA improves glucose oxidation by regulating the PDK2/4-PDHE1α axis

A previous study found that an imbalance between hepatic glucose consumption (glycolysis) and production (gluconeogenesis) in fish limits the efficiency of glucose utilization for energy production (Kamalam et al., 2017). PDKs-PDHE1α is an important enzyme system, which determines the overall rate of glucose disposal, and links the processes of glycolysis with oxidative phosphorylation (Jaswal et al., 2011; Patel et al., 2014; Wu et al., 2000). In the present study, we found that the 4 PDKs (PDK1-4) isoforms depicted tissue expression specificity, similar to results in mammals (Stacpoole, 2017; Wu et al., 2000) and common killifish (Richards et al., 2008). The mRNA and protein expressions of PDK2 and PDK4 were higher than those of PDK1 and PDK3 in the liver, which is an important glucose metabolism organ, in agreement with the results in rat (Wu et al., 2000), killifish (Richards et al., 2008) and zebrafish (Fukuda et al., 2020). Interestingly, DCA inhibited the mRNA expression and protein concentrations of PDK2 and PDK4, and decreased the phosphorylated level of PDHE1α in Nile tilapia liver in the present study. Earlier studies in mammals indicated that DCA specifically inhibited PDKs by binding to the allosteric sites of PDK1-4 (Kato et al., 2007), and increased the activity of PDHE1α

416 through dephosphorylation, which in turn promoted the oxidative utilization of
417 glucose (Klyuyeva et al., 2019; Thoudam et al., 2019). Therefore, the present study
418 showed that DCA also inhibited PDK2 and 4, and increased the content of $^{14}CO_2$
419 release from [1-^{14}C]-glucose oxidation in Nile tilapia fed on a high carbohydrate diet.
420 Glucose catabolism is linked to its transport and the glycolysis process in
421 mammals hepatocytes (Enes et al., 2009). Accordingly, the Mrna expressions of *glut2*,
422 *glut4*, *gk*, *pk* and *pfk* were also up-regulated in fish fed on the DCA3.75 diet in the
423 present study. Furthermore, the DCA3.75 diet also up-regulated the genes related to
424 the TCA cycle (namely *cs*) and the oxidative phosphorylation process (namely *mtcd1*,
425 *sdha* and *nduta9*). These results verified that DCA accelerated the glucose uptake and
426 oxidation in the liver of fish. It should be noted that, the DCA3.75 diet improved
427 growth performance-related indexes with enhanced WG, PER and CR and reduced
428 FCR in Nile tilapia fed on the DCA0 diet in the present study, probably owing to the
429 increased energy supply from glucose oxidation. Taken together, our results indicate
430 that DCA improves the carbohydrate utilization efficiency and growth performance of
431 Nile tilapia by regulating the PDK2/4-PDHE1α axis. These results provide strong
432 evidence that the PDK2/4-PDHE1α axis plays an important regulatory role in glucose
433 oxidation. Therefore, the PDK2/4-PDHE1α axis can be used as a potential regulatory
434 target for improving the carbohydrate utilization in farmed fish.
435 *4.2. Dietary DCA alleviates the high carbohydrate diet-induced glucose intolerance*
436 *by enhancing insulin sensitivity*
437 Insulin regulates glucose homeostasis by suppressing gluconeogenesis and

stimulating glucose utilization (Clemmons, 2006). Accordingly, an impaired insulin function leads to the pathological disorders in the glucose homeostasis in fish (Caruso and Sheridan, 2011). Previous studies in fish have indicated that a long-term intake of the high carbohydrate diets led to insulin resistance in blunt snout bream (Xu et al., 2018) and Nile tilapia (Boonanuntanasarn et al., 2018a; Li et al., 2021). In the present study, the DCA3.75 diet reduced glucose level in the serum of Nile tilapia fed on 450 g/kg carbohydrate (often considered as a high carbohydrate level for Nile tilapia). These results indicate that DCA alleviates the hyperglycemia induced by the intake of high carbohydrate diet. However, the DCA3.75 diet did not increase insulin content in the serum in the normal state and during the GTT test. These results suggest that DCA accomplishes glucose clearance by increasing the insulin sensitivity, rather than promoting insulin secretion. Further evidences indicated that the DCA3.75 diet up-regulated the phosphorylated protein levels of Irβ, Irs1, Pi3k and Akt, which are all involved in the insulin signaling pathway. These results further confirmed our conclusion that DCA improves the insulin sensitivity in Nile tilapia. Similarly, the inhibition or deletion of PDKs in mice also improved glucose tolerance and insulin sensitivity (Thoudam et al., 2019; Wu et al., 2018a; Wu et al., 2018b; Younghoon Go et al., 2016). Therefore, our results suggest that PDK inhibition by using DCA promotes the insulin sensitivity in fish. Fish nutritionists should target the PDK2/4 as a key metabolic regulator for improving the insulin function in farmed fish.

4.3. Dietary DCA increases glycogen synthesis, and inhibits glycolipid conversion

Excess carbohydrate intake in fish usually causes high lipid deposition by

increasing the lipogenic activity, subsequently elicits oxidative stress, inflammation and finally impairs health (Qiang et al., 2016; Rawles et al., 2008). In the present study, the DCA3.75 diet lowered lipid deposition in Nile tilapia, and also reduced the conversion of ^{14}C-glucose to ^{14}C-lipid. Accordingly, the hepatic mRNA expressions of *srebp1*, *fas*, *dgat* and *accα* genes were all down-regulated in Nile tilapia fed on the DCA3.75 diet, verifying the lipogenesis inhibition. Previous studies in mammals reported that increasing hepatic PDH activity by PDK2 inhibition ameliorated hepatic steatosis, and decreased the lipogenesis capacity by regulating the TCA cycle anaplerosis and ketogenesis (Olaniyi and Olatunji, 2019; Younghoon Go et al., 2016). The inhibitory effects of DCA on hepatic fat accumulation in the present study can be explained by 2 mechanisms. First, DCA promotes glucose towards oxidative catabolism rather than acting as the substrate for lipid synthesis. Secondly, DCA attenuates lipid synthesis by improving insulin sensitivity. Therefore, DCA reduces high lipid deposition in fish by promoting the glucose oxidative catabolism and improving insulin sensitivity.

A previous study found that fish respond to high carbohydrate intakes by increasing glycogen synthesis in the liver and muscle (Shi et al., 2018). In the present study, the DCA3.75 diet also increased the conversion of ^{14}C-labled glucose to ^{14}C-labled glycogen, and caused high glycogen deposition in the liver. Accordingly, the Nile tilapia fed on the DCA3.75 diet up-regulated the hepatic mRNA of *gs*. In addition, a previous study reported that glycogen synthase was inhibited by the increased phosphorylated Gs3kβ protein content (King et al., 2020). Gs3kβ was also

inactivated by insulin signaling through phosphorylation of an N-terminal domain serine residue (Patel et al., 2008). In the present study, we found that the DCA3.75 diet activated insulin signaling pathway, and then increased the phosphorylation level of Gs3kβ. This inhibited Gs3kβ, stimulated glycogen synthase activity. These results indicate that DCA stimulates the conversion of glucose into glycogen synthesis, but not into lipid deposition.

5. Conclusion

The present study demonstrated that dietary DCA treatment promotes efficient glucose oxidation and insulin sensitivity in Nile tilapia via inhibiting PDK2/4 and activating PDHE1α. Moreover, dietary DCA administration also improves the ability of Nile tilapia to synthesize glycogen, and inhibits glucose conversion into lipid. The underlying mechanisms are summarized in Fig. 6. This study provides new understandings on the regulatory effects of the PDK2/4-PDHE1α axis in carbohydrate utilization and remodeling the metabolic balance between glucose and lipid in fish. Our study brings forth new nutritional strategies for improving the adaptation of farmed fish towards high carbohydrate diets.

Acknowledgements

The authors appreciate the financial support provided by the National Key R & D Program of China (2018YFD0900400).

References

An R, Tang Z, Li Y, Li T, Xu Q, Zhen J, et al. Activation of pyruvate dehydrogenase by sodium dichloroacetate shifts metabolic consumption from amino acids to glucose in ipec-j2 eclls and intestinal bacteria in pigs. J Agric Food Chem 2018; 66: 3793-3800.

506 Boonanuntanasarn S, Jangprai A, Kumkhong S, Plagnes-Juan E, Veron V, Burel C, et
507 al. Adaptation of Nile tilapia (*Oreochromis niloticus*) to different levels of
508 dietary carbohydrates: New insights from a long term nutritional study.
509 Aquaculture 2018a; 496: 58-65.
510 Boonanuntanasarn S, Kumkhong S, Yoohat K, Plagnes-Juan E, Burel C, Marandel L,
511 et al. Molecular responses of Nile tilapia (*Oreochromis niloticus*) to different
512 levels of dietary carbohydrates. Aquaculture 2018b; 482: 117-123.
513 Caruso M A, Sheridan M A. New insights into the signaling system and function of
514 insulin in fish. Gen Comp Endocrinol 2011; 173: 227-247.
515 Challiss R A J, Espinal J, Newsholme E A. Insulin sensitivity of rates of glycolysis
516 and glycogen synthesis in soleus, stripped soleus, epitrochlearis, and
517 hemi-diaphragm muscles isolated from sedentary rats. Biosci Rep 1983; 3:
518 675-679.
519 Chan C, Krebs E G. Epidermal growth factor stimulates glycogen synthase activity in
520 cultured cells. Proc Natl Acad Sci 1985; 82: 4563.
521 Clemmons D R. Involvement of insulin-like growth factor-I in the control of glucose
522 homeostasis. Curr Opin in Pharmacol 2006; 6: 620-625.
523 Enes P, Panserat S, Kaushik S, Oliva-Teles A. Nutritional regulation of hepatic
524 glucose metabolism in fish. Fish Physiol Biochem 2009; 35: 519-539.
525 FAO, 2020. The state of world fisheries and aquaculture 2020. Sustainability in action.
526 Food and Agriculture Organization, Rome: pp: 206.
527 Folch J, Lees, M., Stanley, G S. A simple method for the isolation and purification of
528 total lipides from animal tissues. J Biol Chem 1957; 226: 497-509.
529 Fukuda R, Marin-Juez R, El-Sammak H, Beisaw A, Ramadass R, Kuenne C, et al.
530 Stimulation of glycolysis promotes cardiomyocyte proliferation after injury in
531 adult zebrafish. EMBO Rep 2020; 21: e49752.
532 Gopal K, Saleme B, Al Batran R, Aburasayn H, Eshreif A, Ho K L, et al. Foxo1
533 regulates myocardial glucose oxidation rates via transcriptional control of
534 pyruvate dehydrogenase kinase 4 expression. Am J Physiol Heart Circ Physiol
535 2017; 313: H479-H490.
536 Gudi R, Melissa M K, Kedishvili N Y, Zhao Y, Popov K M. Diversity of the pyruvate
537 dehydrogenase kinase gene family in humans. J Biol Chem1995; 270:
538 28989-28994.
539 Harris R A, Melissa M , Huang B, Wu P. Regulation of the activity of the pyruvate
540 dehydrogenase complex. Advan Enzyme Regul 2002; 42: 249-259.
541 Hassoun E, Kariya C, Williams F E. Dichloroacetate-induced developmental toxicity
542 and production of reactive oxygen species in zebrafish embryos. J Biochem
543 Mol Toxicol 2005; 19: 52-58.
544 Hemer G I, Mommsen T P, Krogdahl A. Carbohydrates in fish nutrition: Effects on
545 growth, glucose metabolism and hepatic enzymes. Aquacult Nutr 2002 8:
546 175-194.
547 Jaswal J S, Keung W, Wang W, Ussher J R, Lopaschuk G D. Targeting fatty acid and
548 carbohydrate oxidation-a novel therapeutic intervention in the ischemic and
549 failing heart. Biochim Biophys Acta 2011; 1813: 1333-1350.

Jeoung N H, Harris R A. Pyruvate dehydrogenase kinase-4 deficiency lowers blood glucose and improves glucose tolerance in diet-induced obese mice. Am J Physiol Endocrinol Metab 2008; 295: 46-54.

Jin J, Medale F, Kamalam B S, Aguirre P, Veron V, Panserat S. Comparison of glucose and lipid metabolic gene expressions between fat and lean lines of rainbow trout after a glucose load. PLoS One 2014; 9: e105548.

Kamalam B S, Medale F, Panserat S. Utilisation of dietary carbohydrates in farmed fishes: New insights on influencing factors, biological limitations and future strategies. Aquaculture 2017; 467: 3-27.

Kato M, Li J, Chuang J L, Chuang D T. Distinct structural mechanisms for inhibition of pyruvate dehydrogenase kinase isoforms by azd7545, dichloroacetate, and radicicol. Structure 2007; 15: 992-1004.

King B, Li S, Liu C, Kim S J, Sim C. Suppression of glycogen synthase expression reduces glycogen and lipid storage during mosquito overwintering diapause. J Insect Physiol 2020; 120: 103971.

Klyuyeva A, Tuganova A, Kedishvili N, Popov K M. Tissue-specific kinase expression and activity regulate flux through the pyruvate dehydrogenase complex. J Biol Chem 2019; 294: 838-851.

Kuang X, Liu C, Fang J, Ma W, Zhang J, Cui S. The tumor suppressor gene lkb1 is essential for glucose homeostasis during zebrafish early development. FEBS Lett 2016; 590: 2076-2085.

Li L, Li J, Ning L, Lu D, Luo Y, Ma Q, et al. Mitochondrial fatty acid β-oxidation inhibition promotes glucose utilization and protein deposition through energy homeostasis remodeling in fish. J Nutr 2020a; 150: 2322-2335.

Li L, Lu D, Jiang Z, Limbu S M, Qiao F, Chen L, et al. Dietary l-carnitine improves glycogen and protein accumulation in Nile tilapia via increasing lipid-sourced energy supply: An isotope-based metabolic tracking. Aquacul Rep 2020b; 17: 100302.

Li L, Wang Y, Limbu S M, Li J, Qiao F, Chen L, et al. Reduced fatty acid β-oxidation improves glucose catabolism and liver health in Nile tilapia (*Oreochromis niloticus*) juveniles fed a high-starch diet. Aquaculture 2021; 535: 736392.

Limbu S M, Zhang H, Luo Y, Chen L, Zhang M, Du Z. High carbohydrate diet partially protects Nile tilapia (*Oreochromis niloticus*) from oxytetracycline-induced side effects. Environ Pollut 2020; 256: 113508.

Limbu S M, Zhou L, Sun S, Zhang M, Du Z. Chronic exposure to low environmental concentrations and legal aquaculture doses of antibiotics cause systemic adverse effects in Nile tilapia and provoke differential human health risk. Environ Int 2018; 115: 205-219.

Liu C, He A, Ning L, Luo Y, Li D, Zhang M, et al. Leptin selectively regulates nutrients metabolism in Nile tilapia fed on high carbohydrate or high fat diet. Front Endocrinol (Lausanne) 2018; 9: 574.

Livak K J, Schmittgen T D. Analysis of relative gene expression data using real-time quantitative pcr and the $2^{-\Delta\Delta ct}$ method. Methods 2001; 25: 402-408.

Luo Y, Hu C, Qiao F, Wang X, Qin J G, Du Z, et al. Gemfibrozil improves lipid

metabolism in Nile tilapia *Oreochromis niloticus* fed a high-carbohydrate diet through peroxisome proliferator activated receptor-alpha activation. Gen Comp Endocrinol 2020; 296: 113537.

Olaniyi K S, Olatunji L A. Inhibition of pyruvate dehydrogenase kinase-4 by l-glutamine protects pregnant rats against fructose-induced obesity and hepatic lipid accumulation. Biomed Pharmacother 2019; 110: 59-67.

Patel M S, Nemeria N S, Furey W, Jordan F. The pyruvate dehydrogenase complexes: Structure-based function and regulation. J Biol Chem 2014; 289: 16615-16623.

Patel S, Doble B W, MacAulay K, Sinclair E M, Drucker D J, Woodgett J R. Tissue-specific role of glycogen synthase kinase 3beta in glucose homeostasis and insulin action. Mol Cell Biol 2008; 28: 6314-6328.

Pithukpakorn M. Disorders of pyruvate metabolism and the tricarboxylic acid cycle. Mol Genet Metab 2005; 85: 243-246.

Prisingkorn W, Prathomya P, Jakovlic I, Liu H, Zhao Y, Wang W. Transcriptomics, metabolomics and histology indicate that high-carbohydrate diet negatively affects the liver health of blunt snout bream (*Megalobrama amblycephala*). BMC Genomics 2017; 18: 856.

Qiang J, Yang H, Ma X, He J, Wang H, Kpundeh M D, et al. Comparative studies on endocrine status and gene expression of hepatic carbohydrate metabolic enzymes in juvenile gift tilapia (*Oreochromis niloticus*) fed high-carbohydrate diets. Aquac Res 2016; 47: 758-768.

Rawles S D, Smith S B, Gatlin D M. Hepatic glucose utilization and lipogenesis of hybrid striped bass (*Morone chrysops* × *Morone saxatilis*) in response to dietary carbohydrate level and complexity. Aquacult Nutr 2008; 14: 40-50.

Richards J G, Sardella B A, Schulte P M. Regulation of pyruvate dehydrogenase in the common killifish, fundulus heteroclitus, during hypoxia exposure. Am J Physiol Regul Integr Comp Physiol 2008; 295: R979-990.

Schafer C, Young Z T, Makarewich C A, Elnwasany A, Kinter C, Kinter M, et al. Coenzyme a-mediated degradation of pyruvate dehydrogenase kinase 4 promotes cardiac metabolic flexibility after high-fat feeding in mice. J Biol Chem 2018; 293: 6915-6924.

Shi H, Xu C, Liu M, Wang B, Liu W, Chen D, et al. Resveratrol improves the energy sensing and glycolipid metabolism of blunt snout bream *Megalobrama amblycephala* fed high-carbohydrate diets by activating the ampk-sirt1-pgc-1alpha network. Front Physiol 2018; 9: 1258.

Shrestha M K, Sharma R L, Gharti K, Diana J S. Polyculture of sahar (*Tor putitora*) with mixed-sex Nile tilapia. Aquaculture 2011; 319: 284-289.

Stacpoole P W. Therapeutic targeting of the pyruvate dehydrogenase complex/pyruvate dehydrogenase kinase (pdc/pdk) axis in cancer. J Natl Cancer Inst 2017; 109.

Su J, Mei L, Xi L, Gong Y, Yang Y, Jin J, et al. Responses of glycolysis, glycogen accumulation and glucose-induced lipogenesis in grass carp and Chinese longsnout catfish fed high-carbohydrate diet. Aquaculture 2021; 533: 736146.

638 Takubo K, Nagamatsu G, Kobayashi C I, Nakamura-Ishizu A, Kobayashi H, Ikeda E,
639 et al. Regulation of glycolysis by pdk functions as a metabolic checkpoint for
640 cell cycle quiescence in hematopoietic stem cells. Cell Stem Cell 2013; 12:
641 49-61.
642 Tan Q, Wang F, Xie S, Zhu X, Lei W, Shen J. Effect of high dietary starch levels on
643 the growth performance, blood chemistry and body composition of gibel carp
644 (*Carassius auratus* var. Gibelio). Aquacult Res 2009; 40: 1011-1018.
645 Thoudam T, Ha C M, Leem J, Chanda D, Park J S, Kim H J, et al. Pdk4 augments
646 er-mitochondria contact to dampen skeletal muscle insulin signaling during
647 obesity. Diabetes 2019; 68: 571-586.
648 Wahren J, Ekberg K. Splanchnic regulation of glucose production. Annu Rev Nutr
649 2007; 27: 329-345.
650 Wang Y, Liu Y, Tian L, Du Z, Wang J, Wang S, et al. Effects of dietary carbohydrate
651 level on growth and body composition of juvenile tilapia, *Oreochromis*
652 *niloticusxo×O-aureus*. Aquac Res 2005; 36: 1408-1413.
653 Wu C, Satapati S, Gui W, Wynn R M, Sharma G, Lou M, et al. A novel inhibitor of
654 pyruvate dehydrogenase kinase stimulates myocardial carbohydrate oxidation
655 in diet-induced obesity. J Biol Chem 2018a; 293: 9604-9613.
656 Wu C, Tso S C, Chuang J L, Gui W, Lou M, Sharma G, et al. Targeting hepatic
657 pyruvate dehydrogenase kinases restores insulin signaling and mitigates
658 chrebp-mediated lipogenesis in diet-induced obese mice. Mol Metab 2018b;
659 12: 12-24.
660 Wu P, Blair P, Sato J, Jaskiewicz J, Popov K M, Harris R A. Starvation increases the
661 amount of pyruvate dehydrogenase kinase in several mammalian tissues. Arch
662 Biochem Biophys 2000; 381: 1-7.
663 Xu C, Liu W, Zhang D, Cao X, Shi H, Li X. Interactions between dietary
664 carbohydrate and metformin: Implications on energy sensing, insulin signaling
665 pathway, glycolipid metabolism and glucose tolerance in blunt snout bream
666 *Megalobrama amblycephala*. Aquaculture 2018; 483: 183-195.
667 Xu R, Li M, Wang T, Zhao Y, Shan C, Qiao F, et al. Bacillus amyloliquefaciens
668 ameliorates high-carbohydrate diet-induced metabolic phenotypes by
669 restoration of intestinal acetate-producing bacteria in Nile tilapia. Br J Nutr
670 2021: 1-13.
671 Younghoon G, Jeong J Y, Jeoung N H, Jeon J H, Park B Y, Kang H J, et al. Inhibition
672 of pyruvate dehydrogenase kinase 2 protects against hepatic steatosis through
673 modulation of tricarboxylic acid cycle anaplerosis and ketogenesis. Diabetes
674 2016; 65: 2876-2887.
675 Zhang S, Hulver M W, McMillan R P, Cline M A, Gilbert E R. The pivotal role of
676 pyruvate dehydrogenase kinases in metabolic flexibility. NutrMetab 2014; 11:
677 10.

678 **Table 1** The ingredients and proximate composition of the experimental diets.

Item	DCA0	DCA3.75	DCA7.50	DCA11.25
Ingredients, g/kg				
Casein[1]	336.0	336.0	336.0	336.0
Gelatin[2]	84.0	84.0	84.0	84.0
Soybean oil[3]	70.0	70.0	70.0	70.0
Corn starch[4]	450.0	450.0	450.0	450.0
Vitamin premix[5]	10.0	10.0	10.0	10.0
Mineral premix[6]	10.0	10.0	10.0	10.0
$Ca(H_2PO_4)_2$[7]	7.75	7.75	7.75	7.75
Carboxy methyl cellulose[8]	26.0	26.0	26.0	26.0
Choline chloride[9]	5.0	5.0	5.0	5.0
Dimethyl-β-propiothetin[10]	1.0	1.0	1.0	1.0
Butylated hydroxytoluene[11]	0.25	0.25	0.25	0.25
Dichloroacetate (DCA)[12]	0.00	3.75	7.50	11.25
Total	1,000	1,000	1,000	1,000
Proximate composition, % dry matter basis				
Dry matter	92.37	92.44	92.71	92.33
Protein	37.95	37.89	37.96	38.03
Lipid	6.99	6.85	6.98	6.83
Ash	3.31	3.21	3.22	3.30
Nitrogen-free extract[13]	44.12	44.49	44.55	44.17
Available energy, MJ/kg[14]	16.43	16.40	16.40	16.46
DCA[12], g/kg	-	3.02	6.88	10.88

679 [1] Casein: Wan Ling, Changzhou Linghao Biotechnology Co., Ltd., Jiangsu, China.

680 [2] Gelatin: Sangon Biotech (Shanghai) Co., Ltd., China.

681 [3] Soybean oil: Arawana Brand, Yihai Kerry Investments Co., Ltd., Hubei, China.

682 [4] Corn starch: Shijiazhuang Tangtian starch Co., Ltd., Hebei, China.

683 [5] Vitamin premix provided the following per kilogram of diet: 500,000 I.U. vitamin A, 50,000 I.U.

684 vitamin D_3, 2,500 mg vitamin E, 1,000 mg vitamin K_3, 5,000 mg vitamin B_1, 5,000 mg vitamin B_2,
685 5,000 mg vitamin B_6, 5,000 mg vitamin B_{12}, 25,000 mg Inositol, 10,000 mg pantothenic acid,
686 100,000 mg cholin, 25,000 mg niacin, 1,000 mg folic acid, 250 mg biotin, 10,000 mg vitamin C.
687 [6] Mineral premix provided the following per kilogram of diet: 147.4 g $MgSO_4 \cdot 7H_2O$, 49.8 g NaCl,
688 10.9 g Fe (II) gluconate, 3.12 g $MnSO_4 \cdot H_2O$, 4.67 g $ZnSO_4 \cdot 7H_2O$, 0.62 g $CuSO_4 \cdot 5H_2O$, 0.16 g KI,
689 0.08 g $CoCl_2 \cdot 6H_2O$, 0.06 g NH_4 molybdate, 0.02 g $NaSeO_3$.
690 [7] $Ca(H_2PO_4)_2$: Sangon Biotech (Shanghai) Co., Ltd., China.
691 [8] Carboxy methyl cellulose: Shandong Dongda Commerce Co., Ltd., China.
692 [9] Choline chloride: Sangon Biotech (Shanghai) Co., Ltd., China.
693 [10] Dimethyl-β-propiothetin: Sangon Biotech (Shanghai) Co., Ltd., China.
694 [11] Butylated hydroxytoluene: Sangon Biotech (Shanghai) Co., Ltd., China.
695 [12] Dichloroacetate (DCA): Aladdin Biotech (Shanghai) Co., Ltd., China. The actual DCA
696 concentrations were determined by high-performance liquid chromatography.
697 [13] Calculated as 100 - (moisture + protein + lipid + ash).
698 [14] Based on 16.7 MJ/kg protein, 37.6 MJ/kg lipid and 16.7 MJ/kg nitrogen-free extract (NFE).
699

700 **Table 2** Primer sequences for qRT-PCR analysis in Nile tilapia.

Gene name	Sense and antisense primer (5'–3')	GenBank no.
ef1α	F: CTACGTGACCATCATTGATGCC	AB075952
	R: AACACCAGCAGCAACGATCA	
β-actin	F: AGCCTTCCTTCCTTGGTATGGAAT	KJ126772
	R: TGTTGGCGTACAGGTCCTTACG	
pparα	F: CTGATAAAGCTTCGGGCTTCCA	KF871430
	R: CGCTCACACTTATCATACTCCAGCT	
cpt1b	F: AAGGGACGTTACTTCAAGGTG	GQ395696
	R: TCCGACTTGTCTGCCAAGAT	
accβ	F: ACATGCAGTCCATGCTGCGT	XM_003451659
	R: AAATGCCTCTCAAGCCACTCAA	
srebp1	F: TGCAGCAGAGAGACTGTATCCGA	XM_005457771
	R: ACTGCCCTGAATGTGTTCAGACA	
accα	F: TAGCTGAAGAGGAGGGTGCAAGA	XM_005471970
	R: AACCTCTGGATTGGCTTGAACA	
fas	F: TTGAGGATGTGACTATCCACAGGG	XM_003454056
	R: GTCAGGTTTCCGTTCTCCGAAA	
dgat	F: GCTTGAATTCTGTCACCCTGAAGA	XM_003458972
	R: ACCTGCTTGTAGGCGTCGTTCT	
mtco1	F: CTGTTTATCCCCCACTCGCA	LC189956.1
	R: AATAGATGACACCCCGGCCA	
sdha	F: GGTATTCCGTACCGGCTCTG	XM_003443687.5
	R: GTCGGTGTTCCACACAATGC	
ndufa9	F: ACCTTTTGTGCCCTACCCTC	XM_003447056.4
	R: TTTGTCTGGGGTTGTCCAGG	
gk	F: GACATGAGGACATTGACAAGGGAA	XM_003451020.2
	R: CTTGATGGCGTCTCTGAGTAAACC	
pfk	F: AACCTGTGTGTGATTGGAGGTGAT	XM_003441476.2
	R: CGTGATCTTACCGGCTTTAACAAG	
pk	F: CAGCATAATCTGCACCATCGGT	XM_005472621.3
	R: ATGAGAGAAGTTAAGACGGGCGA	
pepck	F: TGGAAGAACAAACCTTGGCG	XM_003448375
	R: TGGGTCAATAATGGGACACTGTCT	
g6pase	F: AGACCTTATTGGTGGGTTCACGA	XM_003448671.4
	R: CTGAAGGACTTCCTGGTCCAGTTT	
fbpase	F: ACCGGACAATAGCGGAAAATACA	XM_003449650.4
	R: TGGCGAATATTGTTCCTATGGAGA	
idh	F: ACGCATCGCTGAGTACGCCTT	XM_003437590.5
	R: AGACCGTCTGACATCCGCATGA	
cs	F: AGCACCACAGTTTACCAG	XM_003438897
	R: AGTGTTGACAAACCCAGA	
glut2	F: CATTGGCATTCTAATCAGCCAGGT	XM_003442884.5
	R: TTGTAATATTGCTGGCGCTCCA	

glut4	F: GCAGGAGGAAAGCCATGCTTATA	XM_003458705.4
	R: ATCATTTCAAAGGAGCGGCAGA	
gs	F: CCTCACTCTGCGCTGTTATTC	XM_013276796.3
	R: CAGCGGCATGCCTTCAGTTT	
pdk1	F: GAGGAGCAGCGTGTCCATAG	XM_003447311.5
	R: AGGTAACTCCTGTCAAAATCCAGA	
pdk2	F: GCAGAGTTCATCCAGACAA	XM_003448725.5
	R: GACCTGTAGTGCTTATCTGAT	
pdk3	F: GTCATGTCATTGCGAAGGGC	XM_005471769.4
	R: CAGAGCCAGCTCCATAAGGTT	
pdk4	F: AATCCACAGCCAGTCACT	XM_003457260.5
	R: GCAGAGTTCATCCAGACAA	
pdhe1α	F: AATCCACAGCCAGTCACT	XM_013264731.3
	R: GCAGAGTTCATCCAGACAA	

ef1α = elongation factor 1 alpha; *pparα* = peroxisome proliferator activated receptor α; *cpt1b* = carnitine palmitoyl transferase 1b; *accβ* = acetyl-coa carboxylase β; *srebp1* = sterol regulatory element binding transcription factor 1; *accα* = acetyl-coa carboxylase α; *fas* = fatty acid synthase; *dgat* = diacylglycerol o-acyltransferase; *mtco1* = mitochondrial cytochrome c oxidase 1; *sdha* = succinate dehydrogenase complex subunit A; *ndufa9* = NADH dehydrogenase [ubiquinone] 1a subcomplex subunit 9; *gk* = glucokinase; *pfk* = phosphofructokinase; *pk* = pyruvate kinase; *pepck* = phosphoenolpyruvate carboxykinase; *g6pase* = glucose-6-phosphatase; *fbpase* = fructose-1,6-bisphosphatase; *idh* = isocitrate dehydrogenase; *cs* = citrate synthase; *glut2* = glucose transporter 2; *glut4* = glucose transporter 4; *gs* = glycogen synthase; *pdk1/2/3/4* = pyruvate dehydrogenase kinase 1/2/3/4; *pdhe1α* = pyruvate dehydrogenase E1α subunit.

712 **Table 3** Antibodies used for western blotting assay.

Antibodies name	Source	Identifier
Pdk2	Abways	CY7193
Pdk4	Proteintech	12949-1-AP
Pdhe1α	Abways	AB3131
p-Pdhe1α (Ser293)	Abways	CY7247
Irβ	Cell Signaling Technology	Cat #3020
p-Irβ (Tyr1345)	Cell Signaling Technology	Cat #3026
Irs1	Abways	CY3428
p-Irs1 (Ser636)	Abways	CY6308
Pi3k	Abways	AB0036
p-Pi3k (Tyr458/199)	Cell Signaling Technology	Cat #4228
Akt	Cell Signaling Technology	Cat #4691
p-Akt (Ser473)	Cell Signaling Technology	Cat #4060
Gsk3β	Abways	AB3168
p-Gsk3β (Ser9)	Abways	CY6248
Gapdh	Huabio	M1310-2

713 Pdk2= pyruvate dehydrogenase kinase 2; Pdk4= pyruvate dehydrogenase kinase 4; Pdhe1α =
714 pyruvate dehydrogenase E1α subunit; Irβ = insulin receptor β; Irs1 = insulin receptor substrate 1;
715 Pi3k = phosphatidylinositol 3-kinase; Akt = serine/threonine kinase; Gsk3β = glycogen synthase
716 kinase 3β; Gapdh = glyceraldehyde-3-phosphate dehydrogenase.
717

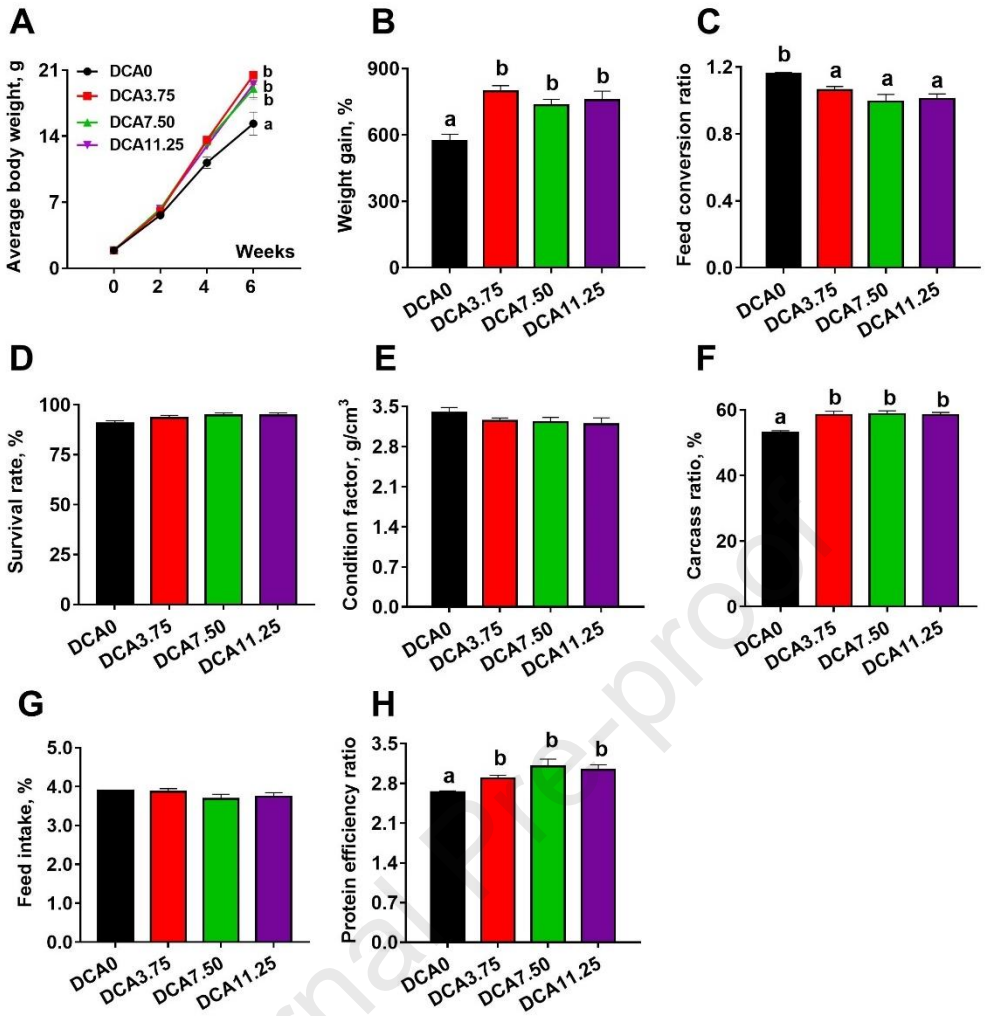

718

719 **Fig. 1** The effects of dichloroacetate (DCA) on growth performance of Nile tilapia. (A) Body weight increase
720 during the 6 wk feeding trial (n = 3); (B) weight gain (n = 3); (C) survival rate (n = 3); (D) feed conversion ratio (n
721 = 3); (E) feed intake (n = 3); (F) protein efficiency ratio (n = 3); (G) condition factor (n = 9); (H) carcass ratio (n =
722 9). Values are means ± SEM. Statistical differences in mean values of all indexes were evaluated by using one-way
723 analysis of variance (ANOVA) followed by Tukey test. [a, b] Different letters indicate a significant difference (P <
724 0.05).

725

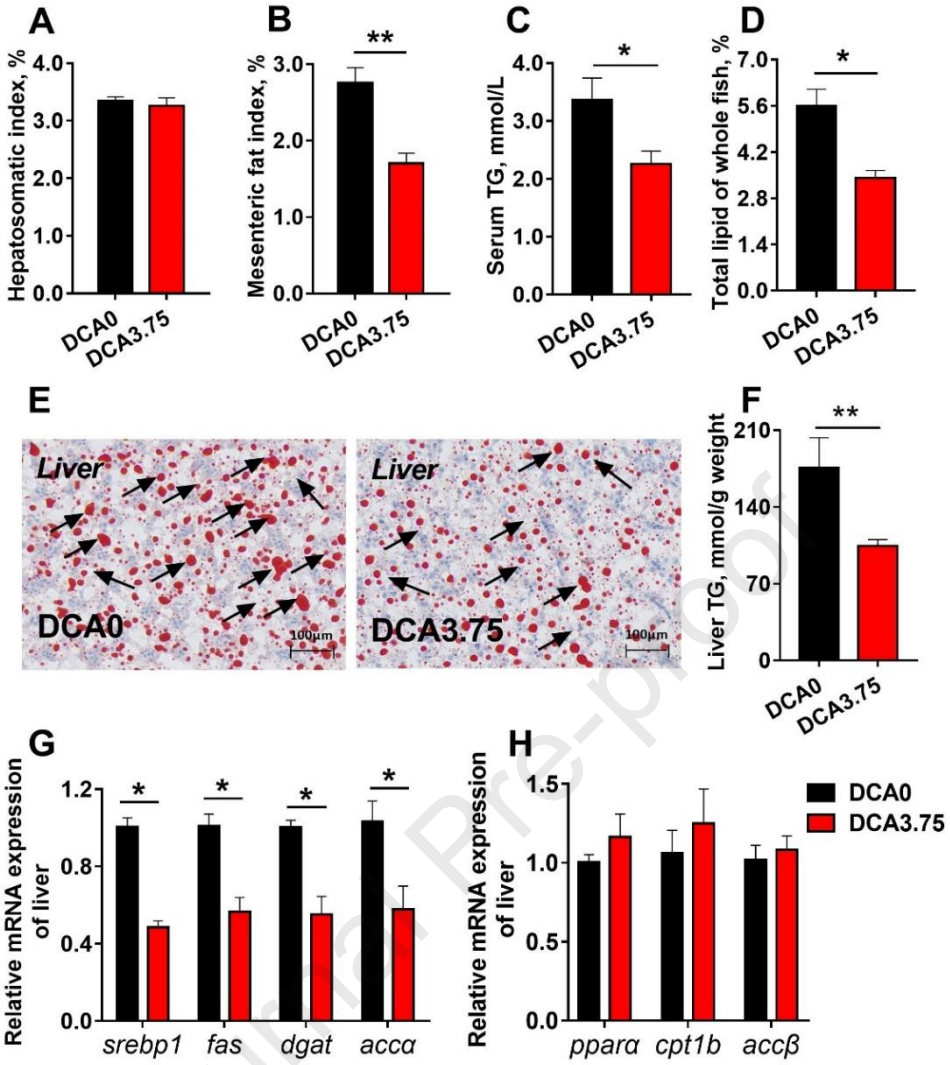

Fig. 2 The effects of dichloroacetate (DCA) on conversion of glucose to lipid in Nile tilapia. (A) Hepatosomatic index (n = 9); (B) mesenteric fat index (n = 9); (C) serum triglyceride (n = 9); (D) total lipid in the whole fish (n = 9); (E) oil red staining of liver tissues (n = 3); (F) liver triglyceride (n = 9); (G–H) the mRNA expression of lipogenesis and lipolysis-related genes in the liver (*srebp1* = sterol regulatory element binding transcription factor 1; *fas* = fatty acid synthase; *dgat* = diacylglycerol o-acyltransferase; *accα* = acetyl-coa carboxylase α; *pparα* = peroxisome proliferator activated receptor α; *cpt1b* = carnitine palmitoyl transferase 1b; *accβ* = acetyl-coa carboxylase β) (n = 9). Values are means ± SEM. Statistical differences in mean values of all indexes were evaluated by using independent t-test. * $P < 0.05$, ** $P < 0.01$.

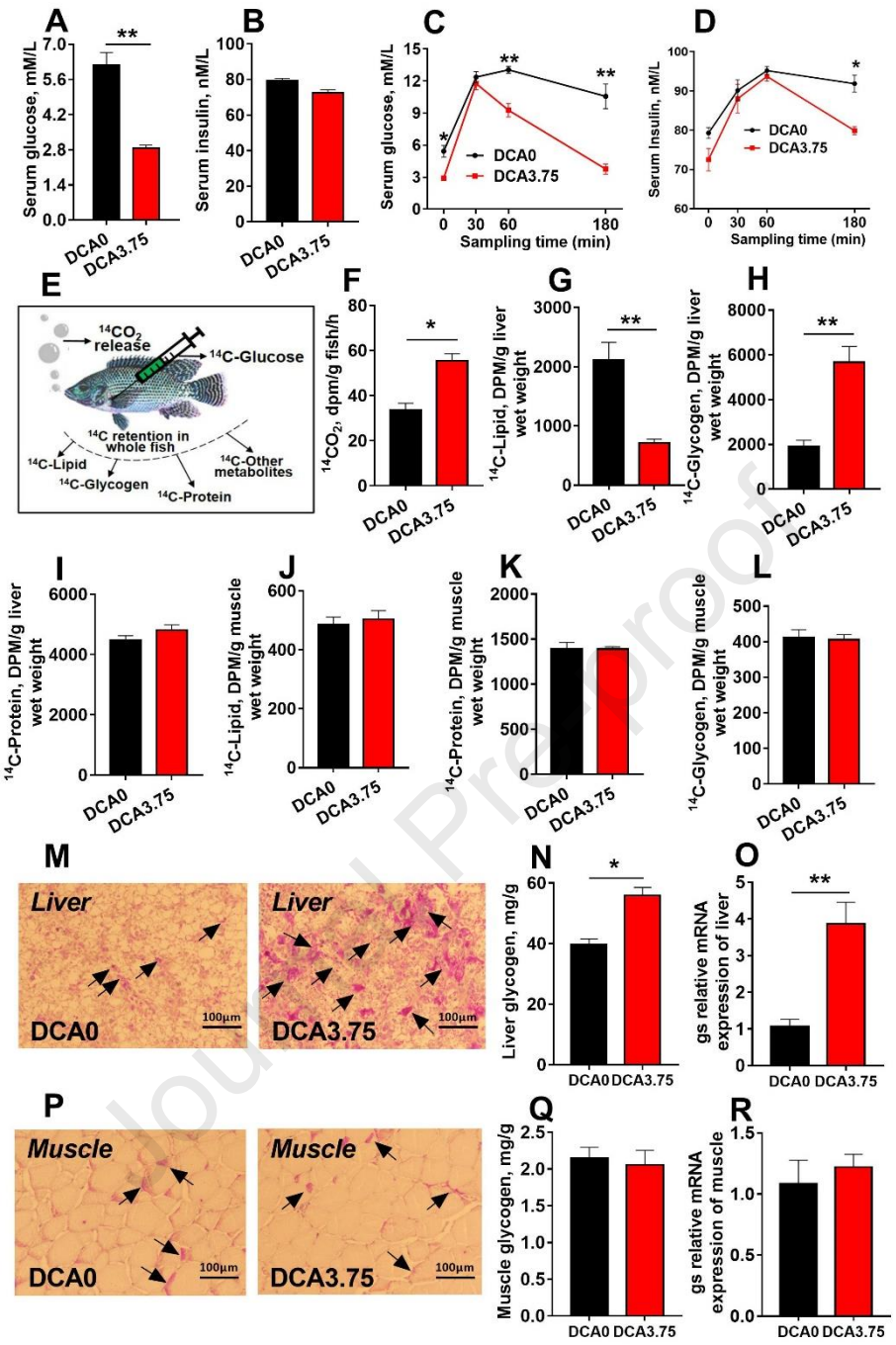

Fig. 3 The effects of dichloroacetate (DCA) on the glucose oxidation utilization in Nile tilapia. (A) Serum glucose (n = 9); (B) serum insulin (n = 9); (C-D) serum glucose and insulin during glucose tolerance test (GTT) (n = 6); (E) schematic diagram of ^{14}C-labelled glucose tracking test in Nile tilapia. (F) carbon dioxide radioactivity released from [1-^{14}C]-glucose oxidation of Nile tilapia (n = 6); (G-I) lipid, glycogen and protein radioactivity of liver during [1-^{14}C]-glucose tracking test of Nile tilapia (n = 6); (J-L) lipid, glycogen and protein radioactivity of muscle during [1-^{14}C]-glucose tracking test of Nile tilapia (n = 6); periodic acid-Schiff (PAS) staining in the liver (M) and muscle (P); glycogen content in the liver (N) and muscle (Q); and the mRNA expression of glycogen synthase in liver (O) and muscle (R) (*gs* = glycogen synthase). Values are means ± SEM. Statistical differences in mean values of all indexes were evaluated by using independent *t*-test. * $P < 0.05$, ** $P < 0.01$.

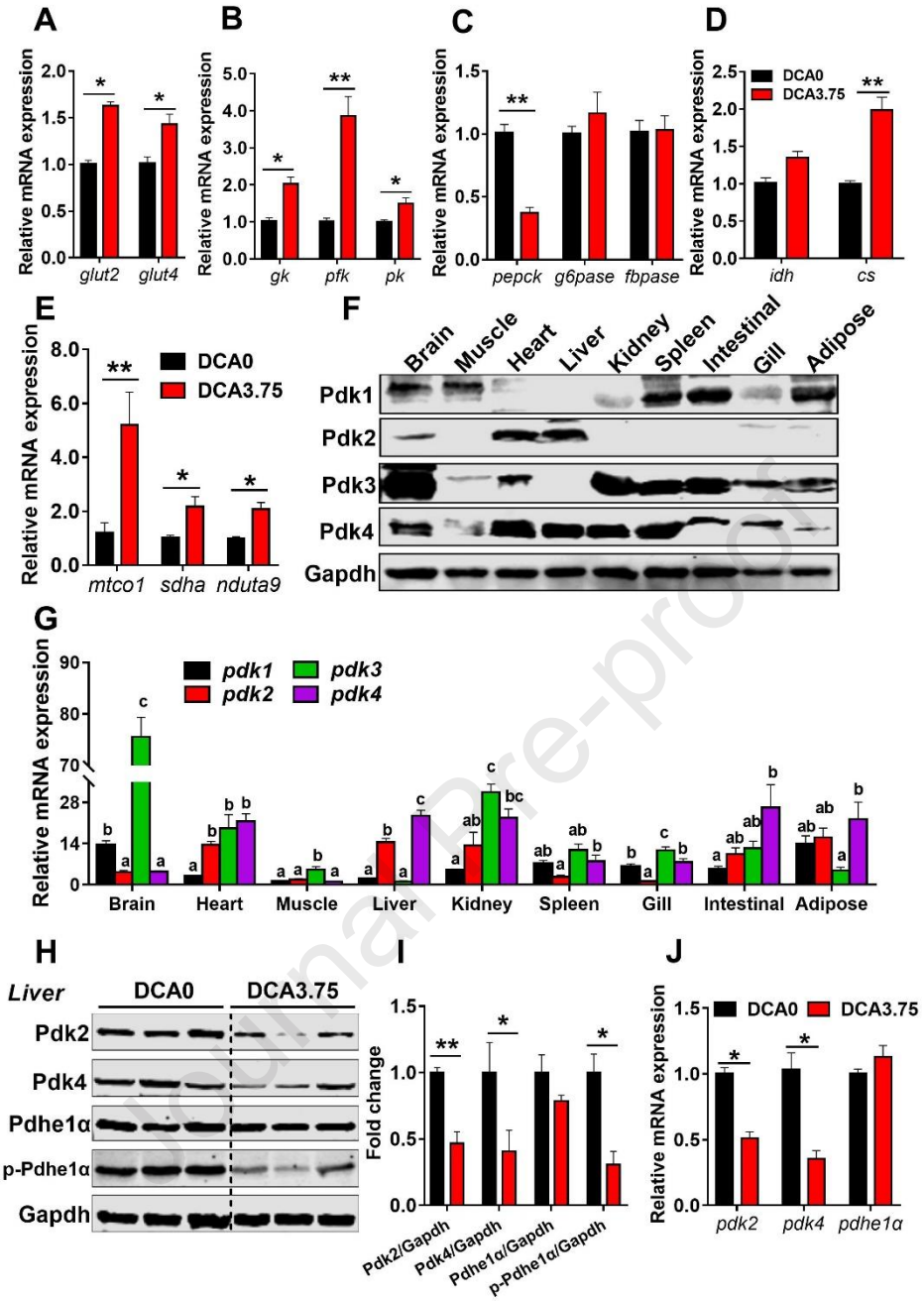

Fig. 4 The effects of dichloroacetate (DCA) on the PDK2/4-PDHE1α axis and expression of genes related to glucose metabolism in Nile tilapia. (A) The mRNA expression of glucose transport-related genes in the liver (*glut2* = glucose transporter 2; *glut4* = glucose transporter 4) (n = 9); (B) the mRNA expression of glycolysis-related genes in the liver (*gk* = glucokinase; *pfk* = phosphofructokinase; *pk* = pyruvate kinase) (n = 9); (C) the mRNA expression of gluconeogenesis-related genes in the liver (*pepck* = phosphoenolpyruvate carboxykinase; *g6pase* = glucose-6-phosphatase; *fbpase* = fructose-1,6-bisphosphatase) (n = 9); (D) the mRNA expression of TCA cycle-related genes in the liver (*idh* = isocitrate dehydrogenase; *cs* = citrate synthase) (n = 9); (E) the mRNA expression of oxidative phosphorylation-related genes in the liver (*mtco1* = mitochondrial cytochrome c oxidase 1; *sdha* = succinate dehydrogenase complex subunit A; *ndufa9* = NADH dehydrogenase [ubiquinone] 1a subcomplex subunit 9) (n = 9); (F-G) mRNA and protein expression patterns of *pdk1*, *pdk2*, *pdk3* and *pdk4* in different tissues (*pdk1/2/3/4* = pyruvate dehydrogenase kinase 1/2/3/4) (n = 6); (H-I) the protein concentrations of Pdk2, Pdk4,

Pdhe1α and p-Pdhe1α in the liver (Pdk2= pyruvate dehydrogenase kinase 2; Pdk4= pyruvate dehydrogenase kinase 4; Pdhe1α = pyruvate dehydrogenase E1α subunit) (n = 9); and (J) the mRNA expression of *pdk2*, *pdk4* and *pdhe1α* genes in the liver (*pdhe1α* = pyruvate dehydrogenase E1α subunit) (n = 9). Values are means ± SEM. Statistical differences in mean values were evaluated by using either one-way analysis of variance (ANOVA) followed by Tukey test (G), or the independent t-test (others except for G). [a, b, c] Different letters indicate a significant difference ($P < 0.05$). ***** $P < 0.05$, ****** $P < 0.01$.

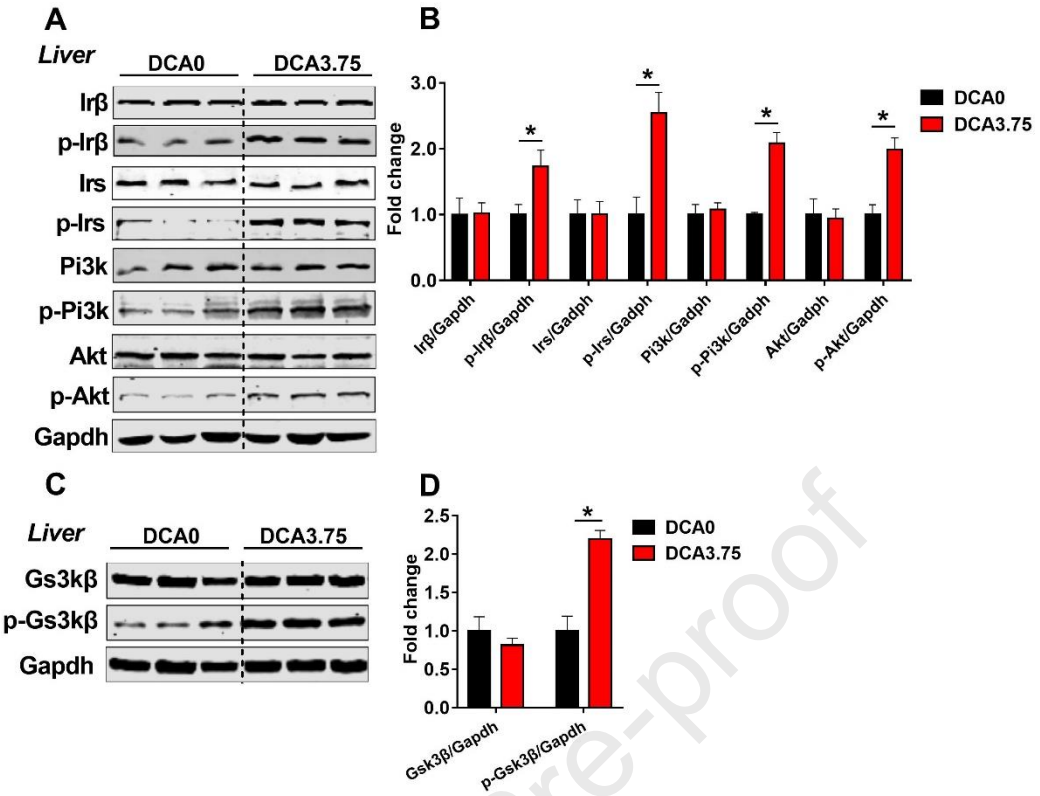

764

765 **Fig. 5** The effects of dichloroacetate (DCA) on the insulin signaling and glycogen synthase kinase 3 beta (GS3Kβ)
766 in Nile tilapia. (A-B) The protein expression of insulin pathway in the liver of Nile tilapia (Irβ = insulin receptor β;
767 Irs1 = insulin receptor substrate 1; Pi3k = phosphatidylinositol 3-kinase; Akt = serine/threonine kinase) (n = 9);
768 (C-D) the protein expression of Gs3kβ and p-Gs3kβ in liver of Nile tilapia (n = 9). Values are means ± SEM.
769 Statistical differences in mean values of all indexes were evaluated by using independent t-test. * $P < 0.05$.

770

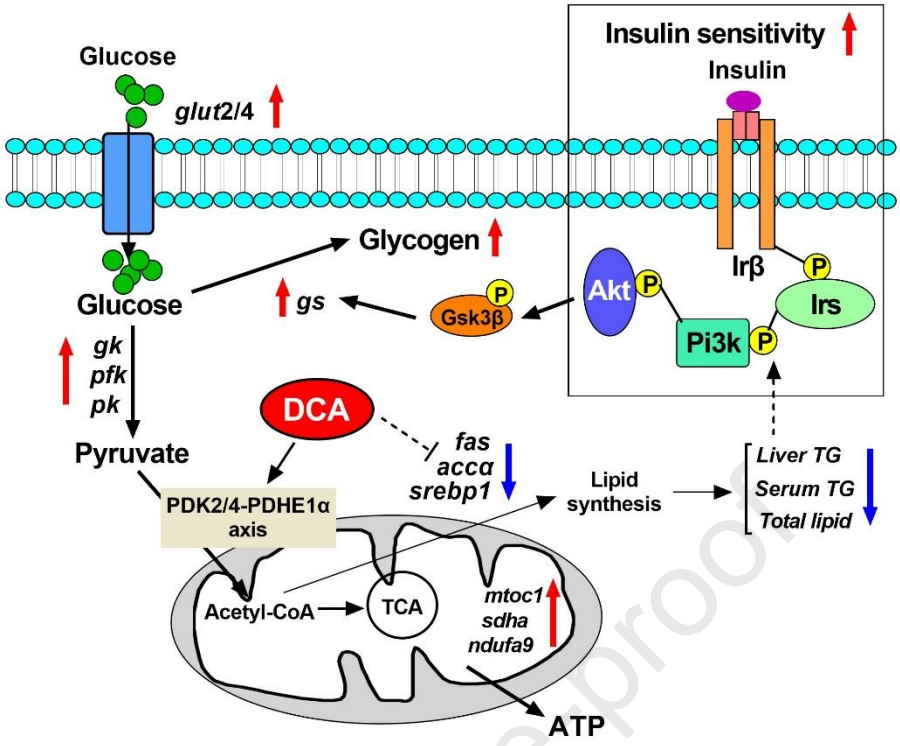

Fig. 6 Summary of the results showing dichloroacetate (DCA) promotes the oxidation utilization of glucose and glycogen synthesis, improves insulin sensitivity, and inhibits glycolipid conversion by regulating the PDK2/4-PDHα axis in Nile tilapia (*gk* = glucokinase; *pfk* = phosphofructokinase; *pk* = pyruvate kinase; *fas* = fatty acid synthase; *accα* = acetyl-coa carboxylase α; *srebp1* = sterol regulatory element binding transcription factor 1; *mtco1* = mitochondrial cytochrome c oxidase 1; *sdha* = succinate dehydrogenase complex subunit A; *ndufa9* = NADH dehydrogenase [ubiquinone] 1a subcomplex subunit 9; *gs* = glycogen synthase; Pdk= pyruvate dehydrogenase kinase; Pdhe1α = pyruvate dehydrogenase E1α subunit; Irβ = insulin receptor β; Irs1 = insulin receptor substrate 1; Pi3k = phosphatidylinositol 3-kinase; Akt = serine/threonine kinase; Gsk3β = glycogen synthase kinase 3β).

Conflict of interest

We declare that we have no financial and personal relationships with other people or organizations that can inappropriately influence our work, and there is no professional or other personal interest of any nature or kind in any product, service and/or company that could be construed as influencing the content of this paper.